Integrated Microfluidic Device for Efficient DNA Extraction Using on-Disk Magnetic Stirrer Micromixer

Amin Dehghan, Ali Gholizadeh, Mahdi Navidbakhsh, Hossein Sadeghi, Esmail Pishbin

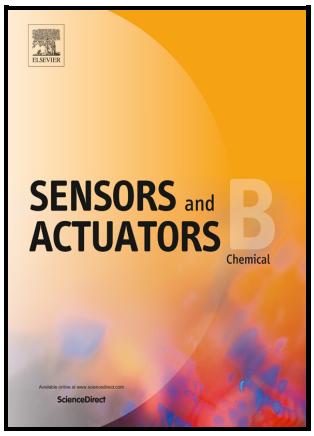

PII: S0925-4005(21)01487-8

DOI: https://doi.org/10.1016/j.snb.2021.130919

Reference: SNB130919

To appear in: *Sensors and Actuators: B. Chemical*

Received date: 25 June 2021
Revised date: 27 August 2021
Accepted date: 11 October 2021

Please cite this article as: Amin Dehghan, Ali Gholizadeh, Mahdi Navidbakhsh, Hossein Sadeghi and Esmail Pishbin, Integrated Microfluidic Device for Efficient DNA Extraction Using on-Disk Magnetic Stirrer Micromixer, *Sensors and Actuators: B. Chemical,* (2021) doi:https://doi.org/10.1016/j.snb.2021.130919

Integrated Microfluidic Device for Efficient DNA Extraction Using on-Disk Magnetic Stirrer Micromixer

Amin Dehghan[1], Ali Gholizadeh[2] , Mahdi Navidbakhsh[1], Hossein Sadeghi[4], Esmail Pishbin[5,*]

[1]School of mechanical engineering, Iran University of Science and Technology, Tehran, Iran

[3]Faculté des Sciences appliquées, Département d'aérospatiale et mécanique, Université de Liège, Belgium

[4]Molecular Genetics Department, Genomic Research Center, Shahid Beheshti University of Medical Sciences, Tehran, Iran

[4] Bio-microfluidics Laboratory, Department of Electrical Engineering and Information Technology, Iranian Research Organization for Science and Technology, Tehran, Iran

*Corresponding Author: pishbin@irost.org

Abstract

Micromixers are essential microfluidic modules for fabricating integrated lab-on-chip devices for point-of-care applications. Ease of fabrication and integration with other fluidic modules, practicability for different viscosities of the solutions, and high mixing efficiencies are the most important characteristics of a suitable micromixer. In this study, a magnetic stirrer on a rotating micro-structured disk is presented to mix liquids of a wide range of viscosities (up to 42 mPa.s) in low

rotational velocities (less than 600 rpm). The concept relies on implementing a small stainless steel rotor aligned on a circular chamber and actuating that by stationary magnets located on the lab frame. The on-disk magnetic stirrer can be implemented in integrated microfluidic platforms without affecting other modules, e.g., valves, to rapidly prepare a homogenous solution in less than 2 seconds. Moreover, high mixing indexes and the considerable viscous stresses generated in solutions make this approach a convenient choice for the cell lysis process. Observations show that DNA yields in the order of 100±15% relative to conventional lysis protocols can be achieved when the stirrer spins at 200 rpm for 1 min.

Keywords: Micromixer, DNA Extraction, Disk, Rotor, Centrifugal microfluidics

Introduction

Automatization of complicated medical laboratory protocols is an advanced application of microfluidic platforms [1][2]. Centrifugal microfluidics has been successfully implemented to carry out standard laboratory protocols, e.g., nucleic-acid-based assays and immunoassays, without needing an external pump [3][4]. Intended fluidic operations are conducted in microstructured chips based on the induced rotational forces and in external forces. Unique specifications for performing complicated biological and chemical assays have made this platform

academically and industrially attractive [4][5][6][7][8][9][10]. Several available centrifugal microfluidic systems on the market are ample evidence of the capability and sustainability of such systems [11].

Pumping, valving, and mixing units are the fundamental operational units required for most of the molecular and cellular biology assays [12][13][14][15][16][17]. Although the Reynolds number of the fluid flow in centrifugal microfluidics is relatively higher than the other types of microfluidic platforms, e.g., pressure-driven, the artificial gravity applied on the liquid is a limiting factor for achieving efficient mixing [18]. The micromixers are intended to effectively mix different solutions in the minimum space and time using in low hardware settings. The active and passive mixing methods in centrifugal microfluidics can be categorized into chamber-based and channel-based types [18]. The latter takes the advantage of injecting the liquid solutions into a microchannel to enhance the interfacial areas and consequently the diffusion rate [19][20]. It has been shown that High mixing efficiencies can be achieved using the zigzag or serpentine shapes for the microchannel [21][22]. Radially outward direction of the applied centrifugal force necessitates the alignment of the in-channel mixers in the radial direction manner. As a shortcoming, employing several mixing structures for multi-step biochemical protocols cause a considerable occupation of the disk's space. Segmented flow-based mixing is an advanced type of mixing that has been recently presented for

centrifugal microfluidics[23]. The method relies on the secondary flow forming in slug flows in spiral microchannels. The presented multiphase mixing strategy makes it possible to mix the liquids in a compact space, however, performing multiple mixing steps may be challenging.

On the other hand, the chamber-based technique handles the mixing in a compact region through active and passive actuation techniques. The shaking technique is a well-known example of this kind of mechanism that liquids are mixed in a chamber by applying an intermittent velocity profile on the disk [24]. Moreover, a reciprocating flow of the liquids between two chambers using the pressurized air and centrifugal inertial forces is successfully implemented in different studies [25][26]. Requiring relatively high acceleration/deceleration rates and particular spinning profiles for an adequate mixing efficiency are the main drawbacks of these methods. Bubble mixing as a rapid and robust strategy requires a considerably complex and spacious microfluidic network [18]. The thermal or fluidic compartments, implemented for the generation of the gas bubbles, occupy a considerable part of the available space on the disk. Despite the complexities added to the system, the active mixing approaches have shown more versatility and controllability compare with passive techniques [27]. The operation is based on forces applied by external sources such as electrical, magnetic, and mechanical actuators [24]. Mechanical micromixers are suitable choices for some advanced

biological applications such as cell lysis [28][29]. The induced flow shear forces in liquid media raise the cell lysis [30][31][32] efficiency. So, the total reaction time can be decreased to conduct the biomedical test more rapidly.

This study aims at presenting a mixing approach based on using a spinning rotor in a circular chamber to mix available liquids. Small permanent magnet(s) fixed underneath the rotating microfluidic chip are responsible for rotating the rotor. The method features the minimum usage of the available space on the cartridge and operating at constant spinning speeds. These characterizations make the presented strategy a suitable candidate for multi-step biological/chemical assays. Magnetic mixers are widely used in laboratories for mixing bulk liquid solutions. Furthermore, similar approaches have been used in microfluidics for pressure-driven platforms by using a rotating magnetic actuator underneath a chip containing a stainless steel rotor [33][34][35]. Alternatively, some research groups have used the concept of actuating the magnetic particles preloaded into a reaction chamber [24][36][37]. In particular, in a centrifugal microfluidic system, magnetic beads are actuated by permanent magnets to enhance advection in the liquid solution[24]. The system has been successfully used to rapidly mix aqueous solutions, however, there is no evidence reporting the applicability of the magnetic beads for mixing the liquids of higher viscosities. Uncontrolled movement of the beads in the chamber may cause the malfunction of the other microfluidic modules

in an integrated microfluidic system. For instance, components or materials of the mechanical or wax valves can be interrupted by small beads [38]. Besides, a complete separation of the particles is not usually possible and in cases that the optical measurement is conducted, the accidental distribution of the particles can be a source of error. The on-disk magnetic stirrer introduced in this study merges the concept of magnetic stirrer into the centrifugal microfluidics for the first time. Arising from the continuous spinning of the disk, the rotation of the stirrer can be accomplished using some permanent magnets fixed in particular locations. The rotor is a fully separated component so its rotation and position can be controlled. Therefore, some above-mentioned challenges related to the magnetic beads can be effectively addressed. The experiments show that the small spinning rotor is capable to mix liquids of a wide range of viscosities when the disk is constantly rotating at a relatively low rotational speed. Considering high mixing efficiencies, the on-disk magnetic stirrer is also utilized for cell lysis. Microfluidic platforms are useful devices for sample preparation in molecular biology[39][40][41]. A considerable DNA extraction out of the whole blood sample is achieved. as a result of simultaneous mechanical and chemical cell lysis

Operational principle

Figure 1a illustrates the schematic of the presented concept. A rotor is mounted into a circular chamber on a rotating disk. To actuate the rotor, the magnets are

fixed at specific radial distances from the disk's rotational axes. The rotor's motion is the result of the applied external forces, including the centrifugal force and magnetic force. At the same time, the hydrodynamic resistant force affects how the rotor rotates in a small container full of liquid. When the rotor nears the permanent magnet, it moves in a direction towards the disk's center. Figure 1b shows the fluctuation of the rotor in a filled chamber with dyed water. The movement of the liquid and bubbles inside is evident as the result of the rotor's oscillation. The size of the rotor should be adjusted to the space available, where narrow circular chambers are selected as the mixing chambers. Here, a 30mm column of Neodymium iron boron (NdFeB) magnets is positioned underneath the microfluidic disk at a vertical distance of 2 mm. The rotor is 5mm in radius and 0.5 mm in thickness. To achieve at least one complete rotation of the rotor in the chamber in one rotation of the disk, the magnet(s) should be arranged in a particular way about the rotation axis. The details of the arrangement of the magnet(s) are presented in the supplementary information, part D. The rotational motion of the rotor causes considerable chaos in liquid bulk due to no-slip conditions and so dramatically reduces the mixing time. The applied force magnitude and the flow convention mainly depend on the rotational speed of the rotor and the viscosity of the liquid.

Numerical modeling of the magnetic rotation

The rotor's motion in the chamber depends on the externally applied forces consist of the magnetic force and the centrifugal force besides the drag force caused by the liquid within the chamber. The applied centrifugal force on the rotor ($\vec{F}_{\omega}$) can be calculated as:

$$\vec{F}_{\omega} = -\mathrm{rho_B} \times V_B \times \vec{\omega} \times (\vec{\omega} \times \vec{R}) \qquad (1)$$

Where $\mathrm{rho_B}$ is the density of stainless steel and V_B stands for the total volume of the rotor. ω and R are the rotational speed of the disk and the average distance from the center of the disk respectively.

In the absence of magnetic force, the rotor poses an equilibrium position. the rotor geometry and rotational speed of the disk are the main parameters that determine this position. Similarly, if the rotor experiences a constant magnetic field, the rotor's position does not change during the rotation. Note that the position we are talking about is the relative position of the rotor in the rotating coordinates. However, using one (or several) permanent magnets in the specific positions about the rotation axis is a solution to apply an actuation force to rotate the rotor. Figure 2 shows the results of numerical simulations on the Comsol Multiphysics 5.3 (Comsol Inc., United States) for evaluation of the magnetic field Computations is conducted for a 3 dimensional model in a time-dependent approach. The disk is

considered to rotate 200 rpm in a clockwise direction. The material of the blade is stainless steel. The magnetic susceptibility is 0.11 which was measured by vibrating sample magnetometer (7400 Series VSM, Lake Shore Cryotronics, Inc, USA). In addition, the magnetic permeability of the material was 1.25×10^{-6} N/A^2. For precisely measuring the density of the rotor, the mass and the volume of the blade were measured as 1.1×10^{-4} kg and 1.43×10^{-8} m^3 respectively. So, 7700 kg/m^3 was used as the density of the material in the simulations. This rotor is exposed to a magnetic field caused by a stack of magnets with a magnetic density of 1.3 T. The magnets were located at a radial distance of 52 mm relative to the center of the disk. The vertical distance between the magnets and the bottom surface of the disk was 2 mm. A mesh independency check showed that the selection of about 8 million tetrahedral elements causes reliable simulation results.

The simulations results indicated in figure 2a show that a specific region on the disk is under the effect of the magnetic field. When the ferromagnetic rotor is placed in a magnetic field $\vec{B}$, the applied magnetic field causes magnetization in the rotor that can be calculated as [24]:

$$\vec{M} = \frac{\left(\chi_b - \chi_{H_2O}\right)}{(1+N_e)\left(\chi_b - \chi_{H_2O}\right)} \frac{1}{\mu_0} \vec{B} \qquad (2)$$

where $\vec{B}$ is magnetic flux density, χ_b is the magnetic susceptibility of the ferromagnetic rotor and the χ_{H_2O} is the magnetic susceptibility of surrounding fluid ranging between 0 and 1. N_e and μ_0 are demagnetization-factor and magnetic permeability respectively. The value of internal magnetization varies based on the power of the magnetic field [33]. In this case, the flux density around the rotor is about 1 T. Rotational speed of the disk determines the elapsed time between force applications. Figure 2b illustrates the applied force diagram on the rotor at a rotation speed of 200 rpm. 5 mN is exerted on a stainless steel rotor with a total volume of $1.43\times10^{-8}m^3$. The magnetic force applied to the rotor can be calculated based on the volume of the rotor V_B and the gradient of magnetic field ($\mathrm{grad}(\vec{B})$) [39][40]:

$$\vec{F}_{mag} = \frac{V_B(\chi_b - \chi_{H_2O})}{\mu_0}.((\mathrm{grad}(\vec{B})).\vec{B}) \qquad (3)$$

Materials and methods

Experimental setup and microfluidic cartridge fabrication

An exclusive experimental setup is made for this study to assess the effects of the operational parameters on the performance of the on-disk magnetic stirrer. Figure 3a illustrates the different components of the experimental setup. An adjustable spinning system is utilized to apply different angular velocities to the microfluidic dick. This system consists of the hardware units and a controlling software. The

details of the driver setup has been presented in our previous paper [42]. A high-speed camera (CASIO EXILIM High-Speed EX-F1) is mounted on top of the microfluidic disk at a specific distance (30 cm) to track the signed rotor location in the chamber. For capturing visible images of the rotating disk, the frame rate of the camera is adjusted based on the rotational speed of the disk between 30 and 60 frames per second. The captured digital images are transferred to the PC for post-processing. Three sets of LED lamps were used to light the rotor's region up to improve the images' quality.

A 400 series stainless steel plate was mounted on a working table to facilitate the movement of the magnets underneath the disk at any desired position. A graded paper between 0 to 360 degrees was stuck over the metal plate placed under the disk to determine the magnets' exact position under the disk. A stack of three neodymium iron boron (NdFeB) magnets was located 2 mm underneath the disk for spinning the rotor in the mixing chamber. Each stack of magnet combination has a 1.3 T magnetic density.

In this study, the PMMA has been selected as the material of the disk. For manufacturing the disk, 3 layers consist of 2 laser-cut sheets of PMMA and a pressure-sensitive adhesive (PSA) were integrated. The details of the microfabrication process are presented in the supplementary information, part A.

Mixing performance

Evaluation of the mixing performance in microfluidic devices is usually performed based on visualization techniques such as color dyes, pH indicators, and fluorescent dyes [21][43][44]. In this study, the grayscale distribution method is used to investigate the effect of different parameters on the mixing quality of the micromixer. The ultimate color of the mixture is considered as the criteria of complete mixing.

To assess the effect of operational parameters on the mixing quality of this micromixer, the normalized standard deviation of this micromixer is calculated. For this purpose, image processing is performed using ImageJ software for obtaining the color intensity of the histogram of the mixed fluids at various times of the mixing process. The profile of pixel intensity distribution on top of the mixing chamber is:

$$\sigma^2 = \frac{\sum_{i=1}^{n}(I_i - \bar{I})^2}{n} \quad (4)$$

Where I_i is the original grayscale intensity value at pixel i, and $0 =< I_i =< 255$ as 8-bit grayscale bitmaps were used. $\bar{I}$ is the averaged value of I_i. The mixing quality based on pixel intensity distribution over the above surface of the mixing chamber is used quantitatively to evaluate the uniformity of mixing, σ_N is defined by:

$$\sigma_N = \frac{\sigma - \sigma_{Min}}{\sigma_{Max} - \sigma_{Min}} \quad (5)$$

Design of Experiments

We developed a design of the experiments to study the effect of different operational parameters on the mixing performance of the on-disk stirrer. The parameters include the viscosity of the liquids, rotational speed of the rotor, and rotor geometry. To cover a wide range of the liquids being used in chemical and biological assays, dyed DI-water is mixed with DI-water and glycerol 75%. This encourages to cover a range of viscosity between 0.89 mPa.s and 41.29 mPa.s (45 times of pure DI water). The dynamic viscosities were measured by a rheometer (Gottfert Capillary Rheograph 6000) at room temperature 25 °C. The black dyed DI-water and water and glycerol75% samples are introduced in equal volumes into the chambers using a sampler.

The on-disk stirrer is designed to rotate at least once in each rotation of the disk with the same rotational speed of the disk. The rotational speeds are limited to a range between 200 rpm and 1000 rpm. The rotor stays at its dynamic equilibrium point without any rotation because the centrifugal force applied to the rotor dominates the magnetic force. The specific arrangement of the magnet(s) can be achieved through the experiments to stimulate and rotate the rotor at each rotational speed. The number of the rotor blades influences the perturbation of the liquid(s) within the chamber and the mixing efficiency. 4 different geometries of

the rotor were designed and employed during the experiments; see Part B in the supplementary information. The thickness of all the rotors is 0.5 mm. In this research, the dimensions of chambers and rotors were designed concerning the volume required for standard DNA extraction protocol. For applications with lower or higher volumes of fluids, the dimensions of chambers and rotors can be scaled smaller or larger.

Cell Lysis process

While liquid color visualization measures the degree of homogeneous distribution of small molecules, the complexity of the mixing process cannot be captured for biochemical applications using this method. Alternatively, some application-oriented methods can be utilized to identify the performance of the presented approach. Since cell lysis is a highly dependent process on the mixing efficiency of the lysis buffer and sample, it is a suitable criterion to determine the efficiency of a mixing strategy. The DNA yield quantifies the performance of the mixing approach. In order to assess the performance of the invented approach, the standard protocol of the manufacturer is applied to the on-disk stirrer mechanism and the conventional mixing in the laboratory. In this regard, the mixing step during the lysis process of a standard DNA extraction protocol is conducted by the following method instead of vortexing.

A microfluidic structure is designed to handle the preparation of the sample in an automated way, to show the ease of integrability of the presented mixing mechanism with other microfluidic modules, see figure 4a. The microfluidic network consists of loading chambers, metering chambers, and the on-disk magnetic stirrer. To achieve maximum efficiency of cell lysis, the metering chamber guarantees using exact volumes of the blood sample and lysis buffer based on the intended test's protocol. The mechanism of this section is based on the overflow mechanism that is shown in figure 4b. In this regard, the liquids are stopped by a burst valve, and the additional volume of the liquid flows into the waste chamber. Based on the protocol, about 100±5 μl of a blood sample is loaded into a loading chamber. After the mixing and lysis process using blood samples and lysis buffer, the DNA extraction is performed off the chip based on the protocol that is presented in detail in the supplementary information, Part C. The DNA yields are measured for the extracted DNA samples employing NanoDrop™. Furthermore, gel electrophoresis is conducted to address the quality of the amplified samples.

Results and discussion

The rotor is intended to rotate one time in each disk's rotation. Several experiments were carried out to find the suitable arrangement of the magnets for each type of the rotors. The details of the magnet positions for other types of blades can be

found in the supplementary information, part D. Figure 5a shows the motion of the 2-blade rotor in 18 different time-lapses in rotational speed 200 pm. These positions are achieved by placing two magnets at 0° and 135°, as shown in the picture. The rotor remains in the intended position by a sharp displacement when they near the magnets. The rotor's moving pattern is the same when the liquid fully occupies the chamber and the magnetic forces thoroughly dominate the drag forces. Two-color indicators (yellow and orange) are stuck on the two blades of the rotor. Also, the radius of the disc (red line) is drawn so that it passes through the center of the mixing chamber as well as the center of the rotor. The red line is considered as a fixed axis on the disk. The rotation of the rotor can be shown by considering the angle changes between the yellow blade of the rotor and the red line. The yellow blade rotates counter-clockwise by about 180° when the position of the mixing chamber is transferred from the position of 0° (position of the first magnet) to the position of 135° (position of the second magnet), just as the disk rotates in a clockwise direction. Then, by continuing to move the mixing chamber towards the 0° position (initial position of the chamber), the yellow blade also continues to rotate in its direction and rotates 180° to returns to its initial position. Therefore, in one rotation of the disk, the rotor rotates a full circle in the mixing chamber. The rotor spinning manner and associated mixing process can is shown in supplementary video1.

Due to dealing with a rotational axis, evaluating the blade's rotation in the rotational coordinate may be complicated. Therefore, we have shown the blade direction in stationary coordinate in figure 5b. In a stationary coordinate, one complete rotation is achieved when the rotor remains at its initial direction during the disk's rotation. The position of the rotor is continuously changed due to applied centrifugal and hydrodynamic. The magnets are responsible to relocate the rotor to its initial condition (that is a horizontal direction in this condition). Based on the results, a complete rotation of the rotor has been achieved, although there are some deviations during the rotation. Adding extra magnets can reduce the deviation. Two different dyed liquids (blue and red) are precisely introduced into the chamber to assess the mixing capability of the spinning rotor by capturing the images during the disk rotation. The rotor's spinning generates a bulk motion in solution causes an adequate mixing of the red and blue liquids. A homogenous mixture appears to be obtained in just one second. The rotor has been rotated about 4 times in this duration based on 200 rpm of rotational speed. Such a rapid mixing was expected due to the liquid volume within the chamber (100 µL), and the high interaction between the rotor and the liquid.

Mixing Characterization

The normalized standard deviation of the pixel intensity for the mixture is used to quantify the mixing process capability. So that, the points near the mean value

report the lower standard deviation and substantially higher mixing efficiency. The effect of the operational parameters on the mixing results has been discussed in the following.

The performance of the on-disk magnetic stirrer to mix the liquids of different viscosities is experimentally investigated on water-water and water-glycerol75%. The rotational speed is set at 200 rpm for the initial experiments. Figure 6a shows a normalized standard deviation based on the color changing of the mixture using a 2-blade rotor. It is worth mentioning that the 1-blade rotor was not able to rotate in the solution of water-glycerol75%. It is due to the relatively lower magnetic force applied by the magnets in comparison to viscous drag forces. The normalized standard deviation of the captured images diminishes to 0 from 1 when the grayscale distributions became more uniform. The efficient mixing occurs in a relatively short time; about 0.92s for the water-water case and 1.6s for water-glycerol75% solution. So the liquids with a wide range of viscosities can be mixed in a very short time based on a rotating stirrer. In the case of high-viscosity solutions, the rotors face rotational resistance in the early stages. While after overcoming the viscous forces, they quickly reach their regular rotation. Achieving a complete mixture after a few rotor spinning can be attributed to sufficient contact between the rotor and liquid during the rotor's rotation.

The rotational speed of the rotor affects the convective mixing of the liquids in the chamber. As the rotor spins faster, the velocity gradient between the layers is increased due to no-slip conditions resulting in a higher shear force. Figure 6b illustrates the normalized standard deviation (NSD) of the mixture at different rotational speeds, i.e., 200, 300, and 400 rpm versus the elapsed time. The graphs show the exponential regression based on the mean values for each condition. The error bars are not shown to prevent the complexity of the graphs. As might be predicted, the mixing time is moderately reduced as the rotational speed increases. For both water-water and water-glycerol 75%, when the rotational speed is increased from 200 rpm to 400 rpm, a reduction in total mixing time is observed by more than 50%. Sloshing of the liquids and the internal flows creates substantial shear stresses on the liquids.

4 different types of geometries are used for the rotors. Figure 6c compares the effect of mixing different dyed DI-water in the reaction chamber using these rotors. No significant improvement in mixing is observed with increasing the number of rotors. Increased number of the blades brings more contact between the solution and the rotor leading to a stronger fluid flow in the mixing chamber to boost the chaotic mixing.

The image processing is conducted in the same regions of the mixing chamber in different spin settings. Dealing with different rotational speeds, the images are

analyzed in different time steps. For ease of comparing results, a regression line is passed based on the non-linear one decay exponential method for each data point. The average R-square is higher than 98%.

One of the drawbacks of the presented mixing method is probable damages to the cells and particles in the biological liquids. High shear forces induced from the considerable rotational speed of the rotors are the reason. In contrast, for applications that require cell destruction, such as the lysis process, this mixing mechanism is desirable.

The performance of the on-disk magnetic stirrer to mix the DI-water with glycerol 75% is qualitatively compared to shake mode mixing and mixing by magnetic beads.

To investigate the effect of shake mode on the mixing of the DI-water with glycerol 75%, this is performed by repeatedly changing the angular velocities between 0 and 480 rpm upon acceleration and deceleration. The maximum acceleration rates of the device are the limitation of this mixing mechanism. The mixing reached its ultimate magnitude after about 4 minutes, while the stirrer micromixer reaches its ultimate magnitude in less than 2 seconds.

To evaluate the performance of magnetic bead-based for mixing of these viscous liquids, an array of permanent magnets fixed underneath the rotating disk and the magnetic beads prefilled into the mixing chamber. It was observed that particles

moving slowly and sediment on one side of the chamber by rotating the disk at 200 rpm. This indicates that the particles do not affect the mixing.

Without rotor, mixing of DI-water with glycerol 75% in 200 rpm rotation of the disk, it was observed that a little of liquids were mixed only by mere diffusion after 20 minutes of disk rotation. It results that a high viscous effect was dominated and prevent the mixing of two liquids.

Evaluation of the DNA extraction

We demonstrate the lysis process on the whole blood as an application of our novel presented mixing technique. Figure 7a gives the percentage of DNA yield relative to the reference magnitude versus discrete times and rotational speed settings. We selected 1, 5, and 10 minutes to consider the processing times effect. The rotational speed is the other factor that may affect the lysis efficiency. The experiments proved that rotational speeds of 200 rpm are practical for complete mixing of the liquids. Higher rotational rates, i.e., 600 and 1000 rpm, are examined to assess the mechanical lysis. Three different tests are conducted for each case. The 2-blade rotor is used regarding the lack of significant differences between the different types of rotors in the mixing efficiency. Besides the arrangement of magnets is simplers for this type of rotor.

Rotor spinning at 200 rpm causes a DNA yield of 100 ± 12% compared with the reference workflow when the sample and lysis buffer are mixed for 1 min. Higher

relative yield levels demonstrate the practicality of the presented technique for the lysis process. Rotor rotation produces considerable shear stress for disruption of the cell's wall due to direct contact with the cells together with the motion of the surrounding lysis buffer. No notable changes are observed when the rotational time is increased for the same rotational setting. Increasing the mixing time to 10 min decreases the yield to 98 ± 10%. For 1000 rpm rotor rotational speed during mixing, a yield is almost equal to the manual reference (99 ± 15%) for 1 min of the whole process. By increasing the mixing time, a slight decrease in the average DNA yield is generated and down to 95 ± 9% for 10 min of reaction time.

It seems if the rotational speed rises, the cell lyses would be enhanced due to elevated shear forces. However, the graph reflects the fact that the maximum cell lysis is achieved at 200 rpm. Regardless of the spinning duration, any speed higher than 200 rpm reduces the amount of extracted DNA. Spinning at 600 rpm leads to the minimum operational efficiency of the device (84 ± 16%). Two reasons can be considered for this reduction. First, a tremendous pushing force is generated at high rotational speeds. The cells are pushed in the outer regions of the mixing chamber and the disruption of the cells is reduces as a result. The more interaction between the particles within the liquid and the spinning rotor, the higher forces are applied to them. Secondly, the centrifugal force proportionally raises with regards to rotational speed, cause the cells to sediment in radially outward positions in the

reaction chamber. Consequently, the homogeneity of the solution composed of particles of high molecular weights is decreased.

Elapsed time is a negative factor on relative DNA yield achieved. It reflects the high shear forces (particularly in high rotational speeds) might have adverse biological effects on the extracted samples [28]. Short process duration and rotational speeds are attractive options for rapid lysis process in low-setting microfluidic systems. The rapid cell lysis following with other procedures require mixing steps, e.g., washing and binding can lead to efficient and fast DNA extraction based on the on-disk magnetic stirrer. It is worth mentioning that applied centrifugal force has a minor effect on extracted DNA due to the low molecular weight of these biological particles. However, these forces can separate the debris and other undesirable suspended materials after the lysis process. The decrease in DNA yield at high rotational speed has been previously reported in some publications [18].

To evaluate the effects of applying different spinning settings on the quality of the extracted DNA strands, they are amplified on a PCR system [45]. The amplified samples are then visualized based on the gel electrophoresis technique.

Figure 7b demonstrates the bands for each test compared to the control condition related to laboratory protocol. In all extraction procedures, a single band was visualized on the agarose gel. The clear bands in the agarose gel show that the

device can extract DNA fragments without degradation. The best amplifications belong to the lowest rotational speed, i.e., 200 rpm that shows sharp bands. Lower brightness in half suitable sample collections represents the more insufficient DNA extracted that is compatible with the DNA yield results. Compared with the control result, relatively smaller fragments of the DNA molecules are produced when the rotor spins at 200 rpm for 1 minute. Durations of 5 and 10 minutes show high similarity with the control results regarding brightness and DNA sizes extracted. In order to compare the results more clearly, a grayscale diagram is extracted from the band using image processing on the ImageJ. In comparison to the control, rotation of the rotor at 200 rpm shows the best extraction output. Finally, the image shows a specific amplification for all tests.

The operation of the on-disk magnetic stirrer is summarized in Table1. According to the table, the highest efficiency for 3 different functions is mixing low and high viscous liquids besides the lysis process. For both viscosities cases, the highest applied rotational speed (400 rpm) and the highest number of blades result in the best mixing performance. In contrast, applying 200 rpm on the rotor leads to the most efficient cell lysis process, where a 2-blade rotor was utilized for all the experiments. The second column presents the simplest possible setting for each condition mentioned above. It is appropriate when lowering the complexity, size, and cost of the system is prime. For instance, complete mixing of the high viscous

liquids caries on a disk rotating at 200 rpm with a 2-blade rotor and 2 magnets. The results suggest that a 2-blade rotor shows an efficient function for the experiments. The last column of the table presents the required time for complete mixing and lysis.

Conclusion

This paper aims at presenting an operational unit in centrifugal microfluidics for efficient conduction of two demanded processes in biological diagnostic tests, i.e., mixing and cell lysis. The platform comprises a stainless steel rotor in a chamber of the intended size and a magnet underneath the rotating microfluidic cartridge. The process is conducted at constant and relatively low rotational speeds in a quiet setting. The module can be easily integrated with other thermal and fluidic units to handle complex fluidic operations for multi-step assays. The mixing techniques are comprehensively characterized by several experiments to analyze the influence of the operational parameters. The results show that the system is capable of mixing high viscous liquids, in orders of 40 Pa.s, with a water-based solution. The mixing efficiency rises when the stainless steel rotor spins faster. A complete mixture of water-based solutions can be achieved in about one second. Mixing some biological liquids might be restricted by this type of mixer regarding the probable effects of the particle. In other cases, the on-disk magnetic stirrer is an ideal choice and a possible alternative for the existing mixing technologies. The main

characteristics consist of versatile mixing function, ease of the setup based on inexpensive hardware, and occupying minimum available space on the cartridge. The device can be implemented for the lysis process when the rotor spinning generates high shear forces. The on-disk magnetic stirrer module is incorporated into a microfluidic system composed of loading, metering, and cell lysis modules for proof of concept. In an automated procedure, the white blood cells are lysed to extract the DNA. The cell lysis process is done based on the standard laboratory procedure and materials. Optical identification of the extracted DNA reports that the system can have the same lysis efficiency in some rotational profiles. The relative DNA extraction (100±15%) was achieved when the disk was spun for 1 minute at 200rpm. This is a desirable condition for accelerating sample preparation for molecular diagnostics with an acceptable extracted DNA quality. Future studies can focus on integrating the presented technique with available microfluidic modules to carry out complicated assays, e.g., Immunoassay and PCR. Moreover, some surface modifications on the rotor may bring new applications for molecular biology assays.

References

[1] J.F. Hess, M. Kotrová, S. Calabrese, N. Darzentas, T. Hutzenlaub, R. Zengerle, M. Brüggemann, N. Paust, Automation of Amplicon-Based Library Preparation for Next-Generation Sequencing by

Centrifugal Microfluidics, Anal. Chem. 92 (2020) 12833–12841. https://doi.org/10.1021/acs.analchem.0c01202.

[2] O. Strohmeier, M. Keller, F. Schwemmer, S. Zehnle, D. Mark, F. von Stetten, R. Zengerle, N. Paust, Centrifugal microfluidic platforms: advanced unit operations and applications., Chem. Soc. Rev. 44 (2015) 6187–6229. https://doi.org/10.1039/c4cs00371c.

[3] H. Xiong, X. Ye, Y. Li, L. Wang, J. Zhang, X. Fang, J. Kong, Rapid Differential Diagnosis of Seven Human Respiratory Coronaviruses Based on Centrifugal Microfluidic Nucleic Acid Assay, Anal. Chem. 92 (2020) 14297–14302. https://doi.org/10.1021/acs.analchem.0c03364.

[4] L. Serioli, T.Z. Laksafoss, J.A.J. Haagensen, C. Sternberg, M.P. Soerensen, S. Molin, K. Zór, A. Boisen, Bacterial Cell Cultures in a Lab-on-a-Disc: A Simple and Versatile Tool for Quantification of Antibiotic Treatment Efficacy, Anal. Chem. (2020). https://doi.org/10.1021/acs.analchem.0c02582.

[5] E. Pishbin, M. Navidbakhsh, M. Eghbal, A Centrifugal microfluidic platform for determination of blood hematocrit level, in: 2015 22nd Iran. Conf. Biomed. Eng. ICBME 2015, 2016: pp. 60–64. https://doi.org/10.1109/ICBME.2015.7404117.

[6] S.T. Rajendran, E. Scarano, M.H. Bergkamp, A.M. Capria, C.H. Cheng, K. Sanger, G. Ferrari, L.H. Nielsen, E. Te Hwu, K. Zór, A. Boisen, Modular, Lightweight, Wireless Potentiostat-on-a-Disc for

Electrochemical Detection in Centrifugal Microfluidics, Anal. Chem. 91 (2019) 11620–11628. https://doi.org/10.1021/acs.analchem.9b02026.

[7] Y. Zhao, Y. Hou, J. Ji, F. Khan, T. Thundat, D.J. Harrison, Sample Preparation in Centrifugal Microfluidic Discs for Human Serum Metabolite Analysis by Surface Assisted Laser Desorption/Ionization Mass Spectrometry, Anal. Chem. (2019). https://doi.org/10.1021/acs.analchem.8b05756.

[8] K. Maejima, Y. Hiruta, D. Citterio, Centrifugal Paperfluidic Platform for Accelerated Distance-Based Colorimetric Signal Readout, Anal. Chem. 92 (2020) 4749–4754. https://doi.org/10.1021/acs.analchem.9b05782.

[9] I. Michael, D. Kim, O. Gulenko, S. Kumar, S. Kumar, J. Clara, D.Y. Ki, J. Park, H.Y. Jeong, T.S. Kim, S. Kwon, Y.K. Cho, A fidget spinner for the point-of-care diagnosis of urinary tract infection, Nat. Biomed. Eng. 4 (2020) 591–600. https://doi.org/10.1038/s41551-020-0557-2.

[10] D. Zohrehvandi, E. Pishbin, M. Navidbakhsh, M. Eghbal, A New Mechanism for the Plasma Separation from Whole Blood on the Lab-on-a-Disk Systems Based on Moment of Inertia Method, in: 2017 24th Iran. Conf. Biomed. Eng. 2017 2nd Int. Iran. Conf. Biomed. Eng. ICBME 2017, 2018. https://doi.org/10.1109/ICBME.2017.8430258.

[11] J. Ducrée, Efficient development of integrated lab-on-a-chip systems featuring operational robustness and manufacturability, Micromachines. 10 (2019). https://doi.org/10.3390/mi10120886.

[12] Y. Ouyang, J. Li, D.M. Haverstick, J.P. Landers, Rotation-driven microfluidic disc for white blood cell enumeration using magnetic bead aggregation, Anal. Chem. 88 (2016) 11046–11054. https://doi.org/10.1021/acs.analchem.6b02903.

[13] S.T. Krauss, M.S. Woolf, K.C. Hadley, N.M. Collins, A.Q. Nauman, J.P. Landers, Centrifugal microfluidic devices using low-volume reagent storage and inward fluid displacement for presumptive drug detection, Sensors Actuators, B Chem. (2019). https://doi.org/10.1016/j.snb.2018.12.113.

[14] R. Burger, D.J. Kinahan, H. Cayron, N. Reis, J. Fonseca, J. Ducrée, Siphon-induced droplet break-off for enhanced mixing on a centrifugal platform, Inventions. (2020). https://doi.org/10.3390/inventions5010001.

[15] A. Naghdloo, E. Ghazimirsaeed, A. Shamloo, Numerical simulation of mixing and heat transfer in an integrated centrifugal microfluidic system for nested-PCR amplification and gene detection, Sensors Actuators, B Chem. (2019). https://doi.org/10.1016/j.snb.2018.12.084.

[16] S. Fakhari, E. Pishbin, M. Navibakhsh, M. Maghazeh, M. Eghbal, Implementing series of dual-chamber units for sequential loading of

the liquids in centrifugal microfluidic platforms, Microfluid. Nanofluidics. 23 (2019). https://doi.org/10.1007/s10404-019-2222-1.

[17] S. Asiaei, S. Fakhari, E. Pishbin, F. Ghorbani-Bidkorbeh, M. Eghbal, M. Navidbakhsh, Demonstration of an efficient, compact and precise pumping method by centrifugal inertia for lab on disk platforms, J. Micromechanics Microengineering. 29 (2019). https://doi.org/10.1088/1361-6439/ab1afe.

[18] S. Burger, M. Schulz, F. Von Stetten, R. Zengerle, N. Paust, Rigorous buoyancy driven bubble mixing for centrifugal microfluidics, Lab Chip. (2016). https://doi.org/10.1039/c5lc01280e.

[19] W.W.F. Leung, Y. Ren, Crossflow and mixing in obstructed and width-constricted rotating radial microchannel, Int. J. Heat Mass Transf. 64 (2013) 457–467. https://doi.org/10.1016/j.ijheatmasstransfer.2013.04.064.

[20] M. Abdi, E. Pishbin, A. Karimi, M. Navidbakhsh, A Comparative Investigation on the Performance of Different Micro Mixers: Toward Cerebral Microvascular Analysis, J. Multiscale Model. 8 (2017) 1650008. https://doi.org/10.1142/s1756973716500086.

[21] Y. Ren, W.W.F. Leung, Flow and mixing in rotating zigzag microchannel, Chem. Eng. J. 215–216 (2013) 561–578. https://doi.org/10.1016/j.cej.2012.09.136.

[22] A. Shamloo, M. Madadelahi, A. Akbari, Numerical simulation of centrifugal serpentine micromixers and analyzing mixing quality parameters, Chem. Eng. Process. Process Intensif. (2016). https://doi.org/10.1016/j.cep.2016.03.017.

[23] E. Pishbin, A. Kazemzadeh, M. Chimerad, S. Asiaei, M. Navidbakhsh, A. Russom, Frequency dependent multiphase flows on centrifugal microfluidics, Lab Chip. (2020). https://doi.org/10.1039/c9lc00924h.

[24] M. Grumann, A. Geipel, L. Riegger, R. Zengerle, J. Ducrée, Batch-mode mixing on centrifugal microfluidic platforms, Lab Chip. 5 (2005) 560–565. https://doi.org/10.1039/b418253g.

[25] Z. Noroozi, H. Kido, M. Micic, H. Pan, C. Bartolome, M. Princevac, J. Zoval, M. Madou, Reciprocating flow-based centrifugal microfluidics mixer, Rev. Sci. Instrum. 80 (2009). https://doi.org/10.1063/1.3169508.

[26] E. Pishbin, M. Eghbal, S. Fakhari, A. Kazemzadeh, M. Navidbakhsh, The effect of moment of inertia on the liquids in centrifugal microfluidics, Micromachines. 7 (2016). https://doi.org/10.3390/mi7120215.

[27] Z. Cai, J. Xiang, H. Chen, W. Wang, A rapid micromixer for centrifugal microfluidic platforms, Micromachines. 7 (2016). https://doi.org/10.3390/mi7050089.

[28] H. Kido, M. Micic, D. Smith, J. Zoval, J. Norton, M. Madou, A

novel, compact disk-like centrifugal microfluidics system for cell lysis and sample homogenization, Colloids Surfaces B Biointerfaces. (2007). https://doi.org/10.1016/j.colsurfb.2007.03.015.

[29] J. Siegrist, R. Gorkin, M. Bastien, G. Stewart, R. Peytavi, H. Kido, M. Bergeron, M. Madou, Validation of a centrifugal microfluidic sample lysis and homogenization platform for nucleic acid extraction with clinical samples, Lab Chip. 10 (2010) 363–371. https://doi.org/10.1039/b913219h.

[30] A. Shamloo, M. Hassani-Gangaraj, Investigating the effect of reagent parameters on the efficiency of cell lysis within droplets, Phys. Fluids. 32 (2020). https://doi.org/10.1063/5.0009840.

[31] R. Nasiri, A. Shamloo, J. Akbari, P. Tebon, M.R. Dokmeci, S. Ahadian, Design and simulation of an integrated centrifugal microfluidic device for CTCs separation and cell lysis, Micromachines. 11 (2020). https://doi.org/10.3390/mi11070699.

[32] A.K. Jahromi, M. Saadatmand, M. Eghbal, L.P. Yeganeh, Development of simple and efficient Lab-on-a-Disc platforms for automated chemical cell lysis, Sci. Rep. 10 (2020). https://doi.org/10.1038/s41598-020-67995-3.

[33] K.S. Ryu, K. Shaikh, E. Goluch, Z. Fan, C. Liu, Micro magnetic stir-bar mixer integrated with parylene microfluidic channels, (2004) 608–613.

[34] L.H. Lu, K.S. Ryu, C. Liu, A magnetic microstirrer and array for microfluidic mixing, J. Microelectromechanical Syst. (2002). https://doi.org/10.1109/JMEMS.2002.802899.

[35] A.K. Agarwal, S.S. Sridharamurthy, D.J. Beebe, H. Jiang, Programmable autonomous micromixers and micropumps, J. Microelectromechanical Syst. 14 (2005) 1409–1421. https://doi.org/10.1109/JMEMS.2005.859101.

[36] Y. Wang, J. Zhe, B.T.F. Chung, P. Dutta, A rapid magnetic particle driven micromixer, Microfluid. Nanofluidics. 4 (2008) 375–389. https://doi.org/10.1007/s10404-007-0188-x.

[37] T.N. Le, Y.K. Suh, S. Kang, A numerical study on the flow and mixing in a microchannel using magnetic particles, J. Mech. Sci. Technol. 24 (2010) 441–450. https://doi.org/10.1007/s12206-009-1107-8.

[38] E.S. Shanko, Y. van de Burgt, P.D. Anderson, J.M.J. den Toonder, Microfluidic magnetic mixing at low reynolds numbers and in stagnant fluids, Micromachines. 10 (2019). https://doi.org/10.3390/mi10110731.

[39] O. Strohmeier, A. Emperle, G. Roth, D. Mark, R. Zengerle, F. Von Stetten, Centrifugal gas-phase transition magnetophoresis (GTM) - A generic method for automation of magnetic bead based assays on the centrifugal microfluidic platform and application to DNA purification, Lab Chip. (2013). https://doi.org/10.1039/c2lc40866j.

[40] O. Strohmeier, S. Keil, B. Kanat, P. Patel, M. Niedrig, M. Weidmann, F. Hufert, J. Drexler, R. Zengerle, F. Von Stetten, Automated nucleic acid extraction from whole blood, B. subtilis, E. coli, and Rift Valley fever virus on a centrifugal microfluidic LabDisk, RSC Adv. (2015). https://doi.org/10.1039/c5ra03399c.

[41] Y.K. Cho, J.G. Lee, J.M. Park, B.S. Lee, Y. Lee, C. Ko, One-step pathogen specific DNA extraction from whole blood on a centrifugal microfluidic device, Lab Chip. (2007). https://doi.org/10.1039/b616115d.

[42] E. Pishbin, M. Eghbal, M. Navidbakhsh, M. Zandi, Localized air-mediated heating method for isothermal and rapid thermal processing on lab-on-a-disk platforms, Sensors Actuators, B Chem. (2019). https://doi.org/10.1016/j.snb.2019.05.039.

[43] C. Shan, F. Chen, Q. Yang, Z. Jiang, X. Hou, 3D multi-microchannel helical mixer fabricated by femtosecond laser inside fused silica, Micromachines. 9 (2018). https://doi.org/10.3390/mi9010029.

[44] S. Wang, X. Huang, C. Yang, Mixing enhancement for high viscous fluids in a microfluidic chamber, Lab Chip. 11 (2011) 2081–2087. https://doi.org/10.1039/c0lc00695e.

[45] A.T. Scott, T.R. Layne, K.C. O'Connell, N.A. Tanner, J.P. Landers, Comparative Evaluation and Quantitative Analysis of Loop-Mediated Isothermal Amplification Indicators, Anal. Chem. 92

(2020) 13343–13353.
https://doi.org/10.1021/acs.analchem.0c02666.

Figures and table

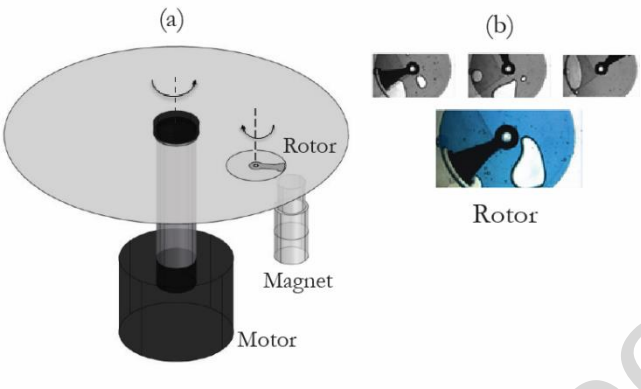

Figure1. Illustration of: a) schematic of the on-disk magnetic stirrer, and b) experiments showing the oscillation of a 1-blade rotor on the circular chamber

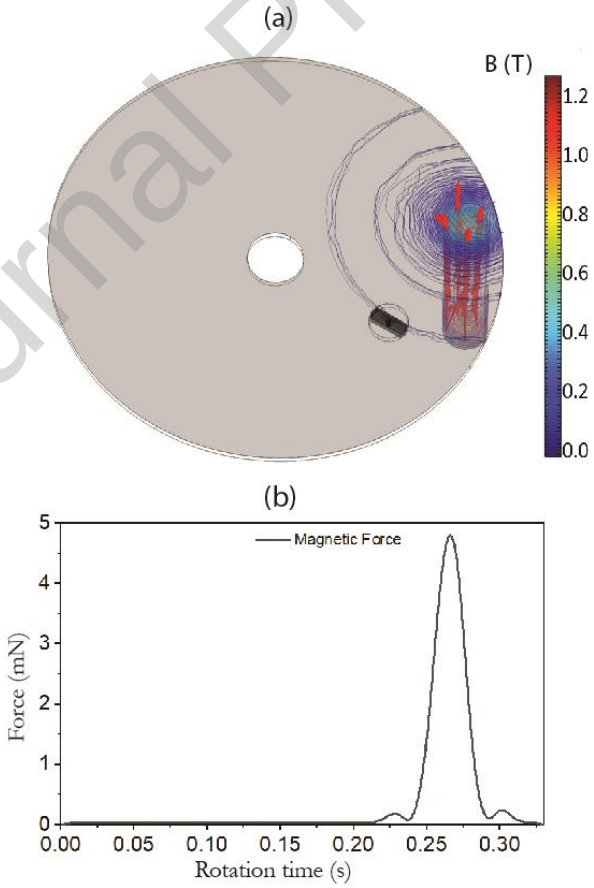

Figure 2. Computational simulations for: a) modeling the magnetic field around the magnets and the rotating disk, and b) the applied magnetic force on the rotor in one rotation of the disk at 200 rpm

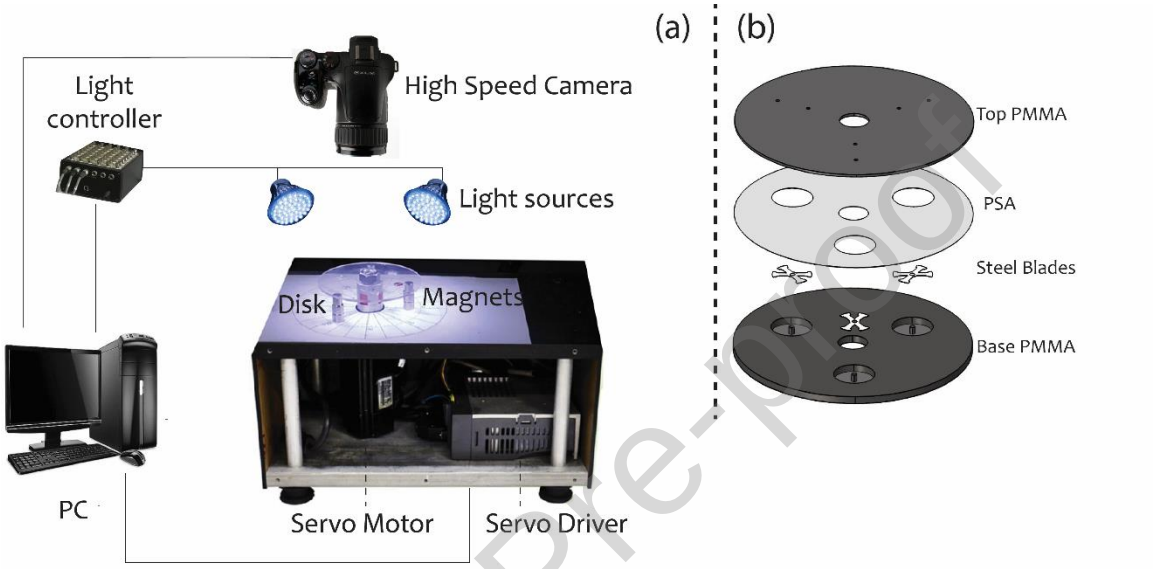

Figure 3. Illustration of: a) different sections of the experimental setup, and b) schematic assembly of the microfluidic disk containing the rotors

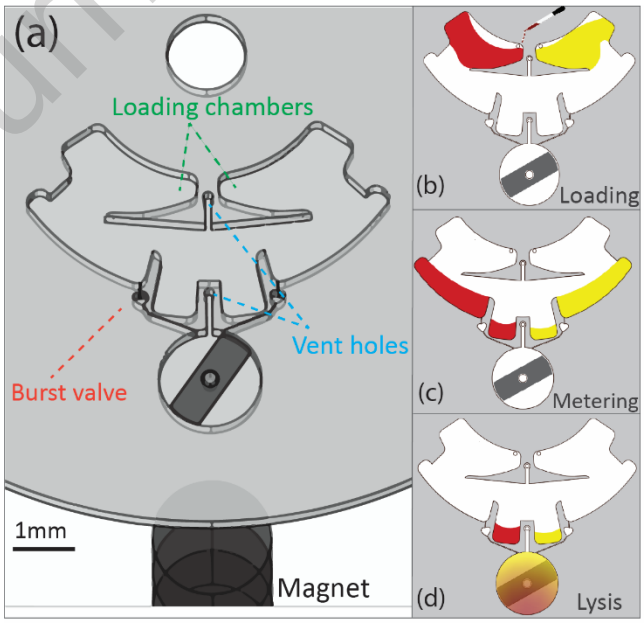

Figure 4. Schematics of: a) the microfluidic structure for automated sampling and cell lysis based on the on-disk magnetic stirrer, b) loading the blood sample and lysis buffer, c) metering step based on overflow mechanism, and d) Lysis process based on the on-disk magnetic stirrer.

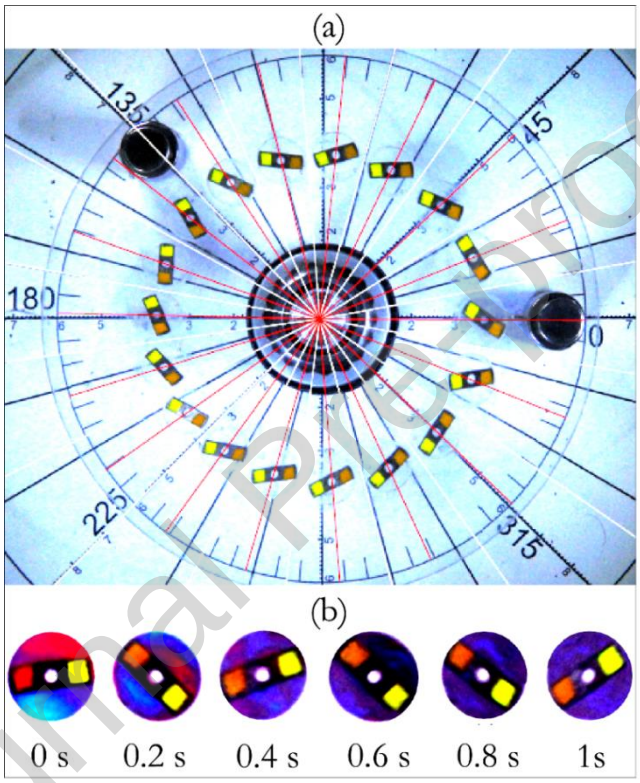

Figure 5. Illustration of a) time-lapses of the rotor's position in the mixing chamber during the rotation of the disk at 200 rpm, and b) the position of the 2-blade rotor in a rotating coordinate and the mixing of different dyed water samples

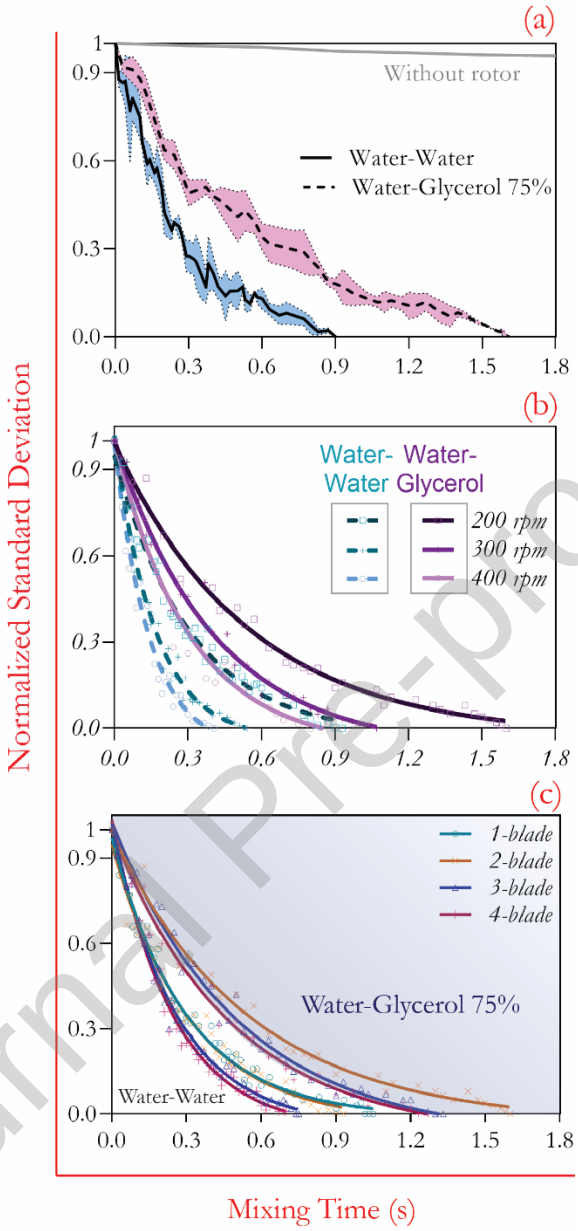

Figure 6. Effect of operational parameters on the mixing efficiency of the on-Disk magnetic stirrer. Illustrating influence of: a) the liquid viscosity based on the water-water and water-glycerol 75% solutions at rotational speed 200 rpm and employing a 2-blade rotor (3 repeats for each test), b) the rotor's spinning speed for water-water and water-glycerol 75% solutions when a 2-blade rotor is used, and c)

the rotor geometry using 4 different types of the rotors for 2 solutions of different viscosities when the disk is rotating at 200 rpm.

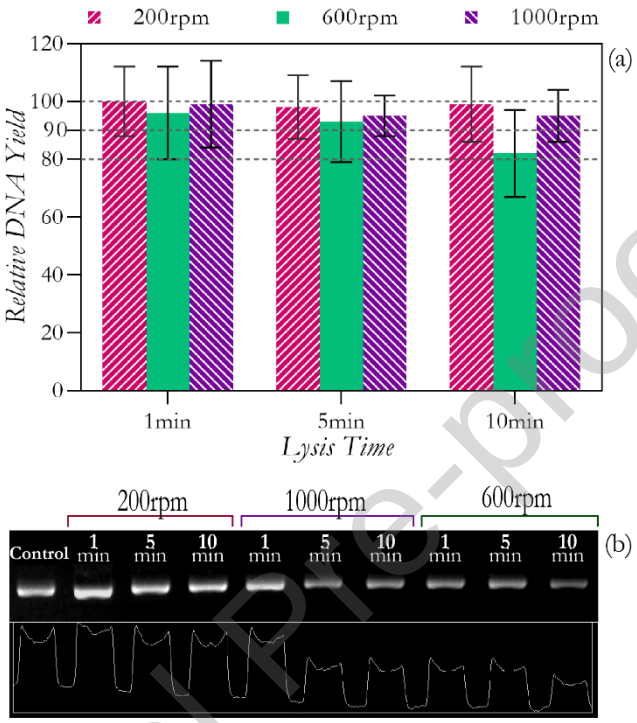

Figure 7. Illustration of the experimental results for: a) Relative DNA yields resulting from cell lysis process implementing on-disk magnetic stirrer in different mixing times and rotational speeds, and b) Gel electrophoresis visualization of the amplified extracted DNA samples based on the different spinning settings of the rotor

Table1. A summary of operational analysis of the rotor's geometry and rotation settings on the mixing and cell lysis processes

	Highest Efficiency	***Lowest Instrumentation***	***2-blade rotor***
Mixing (Low-viscous)	4-blade/400 rpm	1-blade/200rpm/1 magnet	0.92 s
Mixing (High-viscous)	4-blade/400 rpm	2-blade/200rpm/2 magnets	1.6 s
Lysis	2-blade/200rpm	1-blade/200rmp/1 magnets	1 min

Author Biography

Amin Dehghan received his M.S. degree from Iran University of Science and Technology, in 2019. Currently, he is a researcher in school of mechanical engineering at Iran University of Science and Technology. His research work focuses on the digital microfluidics, lab on a disk, and micro fabrication.

Ali Gholizadeh is a research and teaching assistant in the department of aerospace and mechanical engineering at the University of Liège. He recently earned his MS degree in mechanical engineering from Arts et Métiers ParisTech in 2020 after pursuing his research in a microfluidic company in Paris, FLUIGENT SA. His research interests include chip design based on centrifugal microfluidics and smallscale
fluid dynamics with application in biology and clinical diagnostics.

Hossein Sadeghi received his Ph.D. degree from Shahid Beheshti University of Medical Sciences, in 2019. Currently, he is a researcher in SBUMS Genomic Research Center, Tehran, Iran. His research work focuses on the molecular genetics.

Esmail Pishbin received his PhD in 2019 from Iran University of science and technology in mechanical engineering. He is currently working as an associate researcher in field of clinical microfluidics at Heriot- Watt University- the UK. Esmail has several papers for presenting microfluidics solutions for biomedical applications in collaboration with multidisciplinary groups.

Declaration of interests

☒ The authors declare that they have no known competing financial interests or personal relationships that could have appeared to influence the work reported in this paper.

☐The authors declare the following financial interests/personal relationships which may be considered as potential competing interests:

Author contributions

Use this form to specify the contribution of each author of your manuscript. A distinction is made between five types of contributions: Conceived and designed the analysis; Collected the data; Contributed data or analysis tools; Performed the analysis; Wrote the paper.

For each author of your manuscript, please indicate the types of contributions the author has made. An author may have made more than one type of contribution. Optionally, for each contribution type, you may specify the contribution of an author in more detail by providing a one-sentence statement in which the contribution is summarized. In the case of an author who contributed to performing the analysis, the author's contribution for instance could be specified in more detail as 'Performed the computer simulations', 'Performed the statistical analysis', or 'Performed the text mining analysis'.

If an author has made a contribution that is not covered by the five pre-defined contribution types, then please choose 'Other contribution' and provide a one-sentence statement summarizing the author's contribution.

Highlights:

- presenting a Simple and Inexpensive approach for rapid and efficient mixing on microfluidic disc
- capability of mixing of liquids in a wide range of viscosities and volumes in low and constant rotational velocities
- Performing a cell lysis protocol to show the applicability of the technique for implementing in the integrated platforms for molecular diagnostics
- Fully evaluation of the presented method by assessing the effects of different parameters on the performance of the On-Disc magnetic stirrer